

August 1995

TUM/T39-95-11

Nucleon Structure Functions at Moderate Q^2 : Relativistic Constituent Quarks and Spectator Mass Spectrum

S.A.Kulagin^a, W.Melnitchouk^{b*}, T.Weigl^b, W.Weise^b^a *Institute for Nuclear Research, Russian Academy of Sciences, Moscow, Russia*^b *Physik Department, Technische Universität München, D-85747 Garching, Germany.*

Abstract

We present a model description of the nucleon valence structure function applicable over the entire region of the Bjorken variable x , and above moderate values of Q^2 ($\sim 1 \text{ GeV}^2$). We stress the importance of describing the complete spectrum of intermediate states which are spectator to the deep-inelastic collision. At a scale of 1 GeV^2 the relevant degrees of freedom are constituent quarks and pions. The large- x region is then described in terms of scattering from constituent quarks in the nucleon, while the dressing of constituent quarks by pions plays an important role at intermediate x values. The correct small- x behavior, which is necessary for the proper normalization of the valence distributions, is guaranteed by modeling the asymptotic spectator mass spectrum according to Regge phenomenology.

PACS numbers: 12.40.Aa, 13.60.Hb, 25.30.Fj

Typeset using REVTeX

Work supported in part by BMBF.

To appear in *Nuclear Physics A*

*Present address: Department of Physics, University of Maryland, College Park, MD 20742

I. INTRODUCTION

Current deep inelastic scattering (DIS) experiments at HERA are probing the structure of the nucleon at ever smaller values of the Bjorken x variable ($x \equiv Q^2/2M\nu \gtrsim 10^{-4}$), where M is the nucleon mass, and Q^2 and ν the squared four-momentum and energy transfer to the nucleon. The large range of Q^2 available ($4 \lesssim Q^2 \lesssim 3000 \text{ GeV}^2$) allows for quantitative tests of the nature of the evolution of structure functions at these low x [1]. One reason why the small x region is interesting is that it is here that large distance phenomena become relevant, which offers the unique prospect of learning more about the nucleon's non-perturbative structure in DIS.

Before we can fully appreciate the long range structure of the nucleon, there is of course the non-perturbative region at moderate x , but smaller Q^2 ($Q^2 \lesssim 1 \text{ GeV}^2$), which has been the focus of many previous studies, but which still requires quantitative understanding. The significance of this kinematic region is that it reflects precisely the transition between the perturbative and non-perturbative domains of QCD, namely the interface between the parton picture of the nucleon, and the familiar valence quark models of hadrons which successfully describe much of the low-energy phenomenology.

This connection has previously been investigated within phenomenological models of the nucleon, such as bag or non-relativistic quark models [2]. While these efforts have produced some encouraging results, some problems remain, however, in bridging the gap between leading-twist quark distributions calculated within such models, and the experimental structure function data. One problem encountered in most of these approaches has been their failure to correctly describe the $x \rightarrow 0$ behavior of valence quark distributions [3]. This is intrinsically related to the common approximation made in identifying the non-interacting quark system, which is formally on-mass-shell and remains spectator to the deep inelastic collision of the probe with the interacting quark, with a simple diquark, of mass $m_S \sim (2/3)M$. A consequence of this assumption is that to ensure correct normalization, the calculated valence quark distribution must be evolved from extremely low resolution scales,

$Q^2 \sim 0.1\text{--}0.3 \text{ GeV}^2$ [2], where $\alpha_s \sim 1\text{--}3$. At these scales the use of perturbative QCD is rather questionable, and it's not even clear whether adding next-to-leading-order corrections [4–6] is a sensible solution [7]. In this paper we will address the question of whether, and under what conditions, can the inclusion of higher mass spectator states generate sufficiently soft contributions to the valence quark densities so as to allow reliable descriptions of the data when evolved from a scale $Q^2 \sim 1 \text{ GeV}^2$, where perturbative QCD can be used with some more justification.

Our physical framework is assumed to be as follows. At a scale $Q^2 \sim 1 \text{ GeV}^2$ it will be natural to view the nucleon as composed of constituent quark (CQ) “quasi-particles”, which for our purposes will mean quarks having the quantum numbers of QCD (current) quarks, but which acquire a large average mass, $m_Q \sim M/3$, due to their strong non-perturbative interactions. Since this scale is also typically that associated with chiral symmetry breaking, pseudoscalar Goldstone bosons (pions) will in addition play a role. We will therefore assume that the structure of the nucleon seen by a virtual photon with $Q^2 \sim 1 \text{ GeV}^2$ is incorporated within the substructure of the CQs themselves and their pion dressing.

In addition to knowing the internal structure of CQs, one also needs to describe the interaction between CQs in the nucleon, which we parametrize in terms of a relativistic quark–nucleon vertex function. We should state that our aim here is not to calculate the vertex function directly, and it will suffice to adopt a parametrization based on a physically motivated ansatz. Our main aim will be to model the spectral function which describes the non-interacting, spectator quark system, in terms of the degrees of freedom available to us at $Q^2 \sim 1 \text{ GeV}^2$, namely CQs and pions. Within our framework the task of describing the recoil spectator spectrum of the nucleon is reduced to detailing the remnant recoil system that remains after the interaction with the CQ.

The outline of this paper is as follows. In Section II we introduce our model for the spectral function of the spectator quark system. In Section III we discuss the CQ momentum distribution in the nucleon and the low mass spectator spectrum, which gives the leading contribution to the nucleon structure function at large x . The intermediate mass contribu-

tions, which are modeled by dressing the CQs by pions, are described in Section IV. Also discussed is the small- x region of the quark distributions, for which we use a simple model based on Regge phenomenology to describe the large spectator mass continuum contribution to the spectral function. Finally, in Section V we discuss our numerical results and draw conclusions.

II. SPECTRUM OF SPECTATOR STATES

In this Section we outline the basic reasoning behind the need for a detailed description of the spectrum of states that are spectator to the interaction of the photon with a quark in the nucleon (see Fig.1). Let us begin the discussion with the familiar hadronic tensor $W_{\mu\nu}$ which describes deep-inelastic scattering of a virtual photon (momentum q) from a nucleon target (momentum P):

$$W_{\mu\nu}(P, q) = \frac{1}{4\pi} \int d^4\xi \, e^{iq\cdot\xi} \langle P | J_\mu(\xi) J_\nu(0) | P \rangle, \quad (1)$$

where J_μ is the electromagnetic current operator, and the states are normalized such that $\langle P | P' \rangle = 2P_0 (2\pi)^3 \delta^4(P - P')$. For unpolarized scattering, which we consider throughout this paper, $W_{\mu\nu}$ is usually decomposed into two independent structures:

$$W_{\mu\nu}(P, q) = \left(-g_{\mu\nu} + \frac{q_\mu q_\nu}{q^2} \right) F_1 + \left(p_\mu - q_\mu \frac{P \cdot q}{q^2} \right) \left(p_\nu - q_\nu \frac{P \cdot q}{q^2} \right) \frac{F_2}{P \cdot q}, \quad (2)$$

where the structure functions $F_{1,2}$ are expressed as functions of x and $Q^2 (= -q^2)$. In the parton model $F_{1,2}$ become independent of Q^2 (at leading order in α_s), and are related via: $F_1(x) = F_2(x)/2x = 1/2 \sum_q e_q^2 q(x)$, where $q(x)$ gives the probability to find a quark q in the nucleon.

In the usual treatment of inclusive DIS from a nucleon one formally sums over the complete set of intermediate states, which are labeled n in Fig.1, that are spectator to the deep-inelastic collision. In order to reliably calculate structure functions for all $0 < x < 1$ one needs to know the spectator quark spectrum in its entirety, including the contributions

from the large spectator masses. In practice this is quite a challenge to any theoretical approach, and commonly one resorts to approximations which are, however, often valid only in a limited range of x [2].

To elucidate the connection between the quark distribution $q(x)$, calculated at some scale $Q^2 = \mu^2$, and the spectator state n , we can use the so-called dispersion representation of the quark distribution [8,9]. Here $q(x)$ is expressed in terms of the probability density, ρ , of the quark spectator states with invariant mass $s = (P - p)^2$:

$$q(x; \mu^2) = \int ds \int_{-\infty}^{p_{max}^2(s, x)} dp^2 \rho(s, p^2, x; \mu^2), \quad (3)$$

where p is the four-momentum of the struck quark, and

$$p_{max}^2(s, x) = x \left(M^2 - \frac{s}{1 - x} \right) \quad (4)$$

is the kinematical maximum of the quark virtuality p^2 for given x and s . In terms of the amplitude ψ_n describing the absorption of a virtual photon by a quark with momentum \mathbf{p} , this can be written as:

$$\rho(s, p^2, x; \mu^2) = \frac{1}{32\pi^2} \frac{1}{P \cdot q} \sum_n \bar{\psi}_n(\mathbf{P} - \mathbf{p}) \not{q} \psi_n(\mathbf{P} - \mathbf{p}) \delta(s - M_n^2), \quad (5)$$

where M_n^2 is the invariant mass of the intermediate spectator state n , and where formally the amplitude $\psi_n(\mathbf{P} - \mathbf{p})$ is defined via the matrix elements of the quark field operator at the origin $\psi(0)$: $\psi_n(\mathbf{P} - \mathbf{p}) = \langle \mathbf{P} - \mathbf{p}, n | \psi(0) | P \rangle$. An expression similar to (3) holds also for the antiquark distribution $\bar{q}(x)$.

The dispersion representation in Eq.(3) is valid as long as the integrals are convergent. Therefore it is generally assumed that the spectral density vanishes at large quark virtualities p^2 , and that the integration is dominated by contributions from the region of finite p^2 , $|p^2| \lesssim M^2$ [8,9]. Then from Eq.(4) one sees that the smaller the x , the broader the region of s from which $q(x)$ receives contributions. For large x ($x \gtrsim 0.2$), the region of finite $s \lesssim M^2$ is of major importance, and here one can expect models with low-mass spectators, such as diquarks, to be a good approximation. On the other hand, at small x the quark virtuality

p^2 is finite even for large $s \sim M^2/x$. Therefore the quark distribution in Eq.(3) is sensitive to the high-energy part of the spectrum.

The physical origin of the large- s region of the spectator quark spectrum is the high-energy scattering of the virtual $q\bar{q}$ component of the photon from the nucleon. This can be seen by recalling that the quark field operator acting on the target state can either annihilate a quark or create an antiquark in the target. In the former case the matrix element $\psi_n \propto \langle \mathbf{P} - \mathbf{p}, n | a(\mathbf{p}) | P \rangle$ describes the absorption of a virtual photon by quarks with momentum \mathbf{p} , which results in a finite spectrum of intermediate states. On the other hand, the contribution from the antiquark part of the field operator, $\psi_n \propto \langle \mathbf{P} - \mathbf{p}, n | b^\dagger(-\mathbf{p}) | P \rangle$, describes the “external” antiquarks from $q\bar{q}$ fluctuations of the virtual photon and their interaction with the nucleon. The possible antiquark momenta \mathbf{p} are determined by the wave function of the photon and can be as large as the photon momentum \mathbf{q} , leading to a large invariant mass of the antiquark–nucleon system, $s = (P - p)^2 \gg M^2$.

The modeling of the spectral function $\rho(s, p^2, x; \mu^2)$ must of course reflect the resolution scale at which the target nucleon is probed. As mentioned in the Introduction, we will consider ρ at a fixed scale of order $Q^2 = \mu^2 \sim 1 \text{ GeV}^2$. At this model scale, constituent quarks are perhaps the most useful effective degrees of freedom. In a constituent quark picture, the resolution scale can be associated with some average size, R_Q , of the CQ: $\mu^2 \sim 1/R_Q^2$. Results for the color correlation function on a lattice [10] indicate that color fields are confined to a distance of order 0.2 fm. This should also apply to each CQ, and one is led to the estimate $\mu^2 \sim 1 \text{ GeV}^2$. Naturally, at some other scale, CQs may not be the best variables with which to describe the spectral function. However, at $\mu^2 \sim 1 \text{ GeV}^2$, it is known from many other applications that CQs give a good description of the nucleon’s dynamical properties, such as electromagnetic form factors. A natural question to ask therefore is whether CQs can be useful tools in describing DIS from the nucleon, Fig.2.

Within this picture, it will be convenient to break up the spectrum of all possible spectator states into several mass regions, which we now summarize.

- (\mathcal{A}): In a CQ picture, the simplest approximation is to identify the spectator system

which remains after one CQ is removed with a single diquark, with some relatively low mass, $m_S \sim \mathcal{O}(M)$, Fig.3(a). The low- s part ($s \lesssim 1 \text{ GeV}^2$) of the spectral function can then be approximated by:

$$\rho_{\mathcal{A}}(s, x, p^2) = \delta(s - m_S^2) f_{Q/N}(x, p^2), \quad (6)$$

where the function $f_{Q/N}(x, p^2)$, which is now independent of s , is identified with the distribution of constituent quarks in the nucleon with a fraction of the nucleon light-cone momentum x and the invariant mass squared p^2 (see Eq.(7) below) (we omit explicit reference to the scale $\mu^2 \sim 1 \text{ GeV}^2$ from now on). In a relativistic treatment, $\rho_{\mathcal{A}}$ is best described in terms of relativistic quark–diquark–nucleon (QDN) vertex functions. Simple effective models, with constituent quarks as basic ingredients, can be used to calculate the vertex function directly. Note that such calculations are only feasible if the complexity of the task is reduced to that of a few body problem. In other models, where the struck quark is treated as a current quark, the spectator state would have to be very complicated, making even an approximate model solution for the vertex function beyond our present technical ability. Therefore if the spectator state is to be treated as a diquark, then in order to solve for the relativistic vertex function, the struck quark must be a constituent quark.

- (\mathcal{B}): To model the intermediate-mass part ($1 \text{ GeV}^2 \lesssim s \lesssim s_0$) of the spectral function requires going beyond the simplest, single-spectator diquark approximation for the intermediate state. One approach would be to consider higher-Fock state components containing a diquark plus some number of $q\bar{q}$ pairs as spectators. Within the bag model calculations of Ref. [11], for example, these component were modeled in terms of the insertion of an antiquark (or quark), produced from the incoming virtual photon, into the nucleon initial state, which then produced intermediate states with masses of order $(5/4)M$.

At a scale $Q^2 \sim 1 \text{ GeV}^2$, as well as constituent quarks, pseudoscalar Goldstone bosons — pions — also enter as natural degrees of freedom in any effective model description. In a constituent quark picture, therefore, it will be more convenient to model these components in terms of the dressing of CQs by pions, as illustrated for example in Fig.3(b). In practice

we restrict ourselves only the one-pion contributions. One could, in principle, continue the series in the pion number n to large n , hoping to describe the large- s region entirely in terms of pion ladder diagrams. However, taking this route would necessarily mean eventually including dressing due to the heavier meson spectators, as well as from diquarks. A more efficient approach will be to truncate the series at some mass $s = s_0$ (which we take to be $s_0 \sim 2 \text{ GeV}^2$), and describe the large-mass contributions in terms of multi-quark and gluon configurations.

- (\mathcal{C}): To model the large (including asymptotic) mass tail of intermediate states ($s \geq s_0 \sim 2 \text{ GeV}^2$), we describe the amplitude for scattering a $q\bar{q}$ pair from a CQ within Regge theory, which effectively takes into account an infinite set of ladders involving $q\bar{q}$ pairs in the intermediate state, Fig.3(c). The exchange of a Regge trajectory with the intercept $\alpha_R (\approx 1/2)$ leads to imaginary parts of amplitudes rising with energy as E^{α_R} [3]. This energy dependence of the scattering amplitude then gives rise to valence quark distributions which rise at small x as $x^{-\alpha_R}$.

Within the above framework, all three processes \mathcal{A} – \mathcal{C} will be described in terms of CQ parameters, with the basic common unit being the relativistic QDN vertex function. That is, the constituent quark–nucleon interaction is factored out from the hard scattering of the photon with the interacting quark. In the impulse approximation, nucleon DIS can then be viewed as a two-step process, in terms of photon–CQ, and CQ–nucleon subprocesses [12–14]. As we shall see, however, special care has to be given to the fact that the CQ is bound, and thus off-mass-shell.

III. CONSTITUENT QUARK DISTRIBUTIONS IN THE NUCLEON

At the relatively low momentum scales at which a constituent quark model may be relevant, higher twists (i.e. $1/Q^2$ corrections to scaling quark distributions) are bound to play an important role. The final aim, however, is to compare the calculated structure functions with DIS data at large Q^2 ($Q^2 \gtrsim 5 - 10 \text{ GeV}^2$), where higher-twist effects should

be negligible. Therefore it will be sufficient to consider only the leading twist components of the structure function, represented by the “handbag” diagram in Fig.1. At leading twist, the fields that appear in the formal expressions for the current commutators in the forward virtual Compton scattering amplitude are those of point-like, elementary (i.e. current) quarks. In a constituent quark picture, however, the propagator of the quark before it is struck is modeled to be that of a quark with mass $m_Q \sim M/3$ (while the propagating high-momentum quark after the interaction with the photon is a current quark). If one attempts to work with effective, composite degrees of freedom in DIS, a clear and well-defined connection must therefore exist between current and constituent quarks, in particular with respect to the nature of the photon–CQ vertex.

An example of a simple dynamical model in which such a link exists is the Nambu & Jona-Lasinio (NJL) model [15,16]. Here low-momentum gluons are integrated out and absorbed into a local, point-like interaction between quarks, characterized by an effective coupling constant. (Explicit perturbative gluonic degrees of freedom reappear when the calculated quark distributions are evolved to the higher Q^2 appropriate for the DIS region.) The mechanisms used in going from current to constituent quarks are dynamical quark mass generation, involving the scalar interaction of the quark with the Dirac vacuum, together with the spontaneous breaking of chiral symmetry. The connection between current and constituent quark masses is formally quantified via a “gap equation” [15]. Through interactions with quark condensates, (nearly) massless current quarks acquire large constituent masses, of order $m_Q \sim 400$ MeV. (For detailed reviews of the NJL approach see Refs. [16].)

Within this approach a CQ mass therefore appears in the quark propagator, while one still has a simple γ_μ coupling at the photon–quark vertex. There is no form factor suppression at large Q^2 arising from the photon–CQ–current quark vertex. In a relativistic CQ picture, such as that embodied in the NJL model, the diagrams responsible for the CQ form factor are those in which the photon couples to the target CQ via $q\bar{q}$ loops. As $Q^2 \rightarrow \infty$ these rapidly die out, leaving behind only the scaling part associated with the direct coupling of the photon to the CQ. In this way the only difference between scattering from current

and constituent quarks is therefore a renormalization of the quark mass. The dressing of the struck quark propagator is not included, since this would correspond to higher twist corrections.

A. Quark–Diquark–Nucleon Vertex Functions

Having made these remarks, we now turn to the calculation of constituent quark distributions inside the nucleon. Constituent quarks embedded in a nucleon have some characteristic momentum distribution, which is essentially given by the CQ wave function. Within the present approach it is more conveniently expressed in terms of the relativistic quark–diquark–nucleon vertex functions, $\Phi_{QDN}^{(S)}$ (proportional to the product of the wave function and the quark propagator), connecting the nucleon and off-shell quark to the non-interacting (spectator) intermediate state diquark.

In the impulse approximation (i.e. no final state interactions between the struck quark and the residual diquark system) the CQ distribution (see Eq.(6)) can be written:

$$f_{Q/N}^{(S)}(y, p^2) = \int \frac{d^4 p'}{(2\pi)^4} 2\pi \delta\left(y - \frac{p' \cdot q}{P \cdot q}\right) \delta(p'^2 - p^2) \delta((P - p')^2 - m_S^2) \\ \times \frac{1}{2P \cdot q} \text{Tr} \left[\not{q} \mathcal{H}^{(S)}(P, p') \right], \quad (7)$$

where y is the fraction of light-cone momentum of the nucleon carried by the CQ, and the operator $\mathcal{H}^{(S)}$ describes the soft CQ–nucleon interaction. The label (S) refers to the possible spin orientations of the spectator state ($S = 0$ or 1), since any realistic model of the nucleon must incorporate pseudovector as well as scalar diquarks. In terms of the propagators and QDN vertex functions, $\mathcal{H}^{(S)}$ is defined as:

$$\mathcal{H}^{(S=0)}(P, p) = \frac{1}{2} (\not{p} - m_Q)^{-1} \Phi_{QDN}^{(0)}(P, p) (\not{P} + M) \bar{\Phi}_{QDN}^{(0)}(P, p) (\not{p} - m_Q)^{-1}, \quad (8a)$$

for a scalar ($S = 0$) spectator system, and:

$$\mathcal{H}^{(S=1)}(P, p) = \frac{1}{2} (\not{p} - m_Q)^{-1} \Phi_{QDN}^{\alpha(1)}(P, p) (\not{P} + M) \bar{\Phi}_{QDN}^{\beta(1)}(P, p) (\not{p} - m_Q)^{-1} \\ \times \left(-g_{\alpha\beta} + \frac{(P - p)_\alpha (P - p)_\beta}{m_S^2} \right), \quad (8b)$$

for $S = 1$ spectators. Here m_Q is the CQ mass, and the conjugate vertex is defined as $\overline{\Phi}_{QDN}^{(S)} \equiv \gamma_0 \Phi_{QDN}^{(S)\dagger} \gamma_0$.

The trace in Eq.(7) can be separated into terms proportional to the four-momenta P_μ and p_μ :

$$\frac{1}{4} \text{Tr}[\mathcal{H}^{(S)}(P, p) \gamma_\mu] = f_1^{(S)}(p^2) P_\mu + f_2^{(S)}(p^2) p_\mu, \quad (9)$$

where the functions $f_1^{(S)}$ and $f_2^{(S)}$ can be calculated from the QDN vertex. In terms of $f_{1,2}^{(S)}$, the constituent quark distribution function $f_{Q/N}^{(S)}$ is given by:

$$f_{Q/N}^{(S)}(y, p^2) = \frac{1}{8\pi^2} \left(f_1^{(S)}(p^2) + y f_2^{(S)}(p^2) \right). \quad (10)$$

Note that in general the functions $f_{1,2}^{(S)}$ depend on p^2 as well as $P \cdot p$, however the latter is fixed by the δ -function in Eq.(7): $P \cdot p = (M^2 + p^2 - m_S^2)/2$.

Different $S = 0$ and $S = 1$ vertices, as well as a larger pseudovector diquark mass ($m_{S=1} - m_{S=0} \sim 0.2$ GeV), are needed to explicitly break spin-flavor SU(4) symmetry, which is reflected in a softer d quark distribution compared with the u quark distribution [17]. The complete Dirac structure for the vertex $\Phi_{QDN}^{(S)}$ can be written down in terms of a number of independent functions. In particular, one has for the $S = 0$ vertex:

$$\Phi_{QDN}^{(0)}(P, p) = \phi^{(0)} I + \phi_p^{(0)} \not{p}, \quad (11)$$

and similarly for the $S = 1$ case:

$$\Phi_{QDN}^{\alpha(1)}(P, p) = \phi^{(1)} \gamma^\alpha \gamma_5 + \phi_p^{(1)} p^\alpha \gamma_5 + \phi_P^{(1)} P^\alpha \gamma_5 + \dots, \quad (12)$$

although different bases in which to expand $\Phi_{QDN}^{(S)}$ can of course be chosen [18].

In most previous calculations of structure functions involving QDN vertices [19–23] the momentum dependence in $\Phi_{QDN}^{(S)}$ has not been calculated directly, but rather has had to be parametrized, by appealing to DIS data to fix parameters. The approach adopted has been to choose a single form for both the $S = 0$ and $S = 1$ vertices, and adjust the momentum dependence in each, to effectively compensate for the omission of the other structures. For

example, by choosing different shapes for the functions $\phi^{(S=0)}$, one can get similar results whether one uses a structure I [19–21] or one proportional to \not{p} (see also Ref. [23]).

Although the phenomenological approach has been successful in allowing fair descriptions of the nucleon’s valence quark distributions, it is naturally desirable to have stronger theoretical justification for using any particular vertex structure. Recently attempts have been made to calculate $\Phi_{QDN}^{(S)}$ within effective models, notably the NJL model. Here we outline the general approaches used in these calculations — for more details see Refs. [18,24–27]. The simplest ansatz has been to reduce the relativistic three-body calculation to a more tractable, effective two-body problem, by treating the nucleon as a composite of a quark and an elementary diquark [26]. Within this approximation one can solve exactly the Bethe-Salpeter equation for the quark–diquark system using a static approximation for the (local) quark exchange interaction.

Beyond this simplest approximation, the Bethe-Salpeter equation has more recently been solved for the case where the exchanged quark was allowed to propagate between the quark and diquark [18,28]. Ishii et al. [24] and Huang and Tjon [25] have gone further by finding solutions to the covariant Faddeev equation without imposing the constraint that the diquark be elementary. Although only $S = 0$ diquarks were modeled in Refs. [25,26], the authors of Refs. [24,18] have also incorporated pseudovector diquarks in their models for Φ_{QDN} . Note that to describe DIS one only needs the vertex function with an on-shell diquark — solutions to the Bethe-Salpeter or Faddeev equations more generally have both the quark and diquark off their mass shells.

The results of the model calculations [18,28] indicate that the S -wave vertices give the most important contributions to the norm and to the nucleon’s electric charge, which provides some justification for the prescription applied in Refs. [19–23] of using only the leading structures. Furthermore, they show that the shapes of $\phi^{(S)}$ can be reasonably well approximated by simple monopole or dipole functions:

$$\phi^{(S)}(p^2) \propto \frac{(m_Q^2 - p^2)}{(\Lambda_S^2 - p^2)^{n_S}}, \quad (13)$$

with cut-off parameters Λ_S of the order of 1—2 GeV (depending on the precise value of n_S). Such results are not surprising if one's model is to reproduce realistic values for the nucleon's static properties, such as the mass and r.m.s. radius. Note the presence of the zero in the numerator in Eq.(13) at $p^2 = m_Q^2$, which has the role of canceling the quark propagators in $f_{Q/N}^{(S)}$. In principle the quark propagators in Eq.(7) could develop unphysical poles in the kinematically allowed region if the sum of quark and diquark masses falls below the nucleon mass, meaning that the nucleon could freely disintegrate into its constituents. As such the form factor in Eq.(13) reflects the underlying dynamics that are responsible for the bound state of the nucleon. Similar results have been reported for the quark–antiquark–meson vertex function in Ref. [29].

Note that Λ_S is not related to the intrinsic NJL cut-off, Λ_{NJL} . By treating scalar or pseudovector diquarks as quasi-particles, with effective boson propagators $\propto ((P - p)^2 - m_S^2)^{-1}$, one renders all loop integrals appearing in the calculation of the Bethe-Salpeter amplitudes finite, without any need to introduce ultra-violet cut-offs as regulators. This can be easily seen by counting inverse powers of momentum running through the quark–diquark legs. The cut-off Λ_S is therefore only an indicator of the “hardness” of the QDN vertex, or the “size” of the quark–diquark configuration in the nucleon.

For the scalar vertex (11), the S -wave structure $\Phi_{QDN}^{(0)} = I \phi^{(0)}$ [20,21] in Eq.(7) gives for the functions $f_{1,2}^{(0)}$:

$$f_1^{(0)}(p^2) = \frac{1}{2} \frac{|\phi^{(0)}(p^2)|^2}{(m_Q^2 - p^2)}, \quad (14a)$$

$$f_2^{(0)}(p^2) = \frac{|\phi^{(0)}(p^2)|^2}{(m_Q^2 - p^2)^2} (m_Q M + P \cdot p). \quad (14b)$$

Note that an equivalent result is obtained from the structure \not{P} , or $(I + \not{P}/M)/2$, which would be the leading one in the non-relativistic limit [18]. With the pseudovector vertex structure: $\Phi_{QDN}^{(1)} = \gamma_5 \gamma_\alpha \phi^{(1)}$ one has:

$$f_1^{(1)}(p^2) = \frac{1}{2} \frac{|\phi^{(1)}(p^2)|^2}{(p^2 - m_Q^2)} \frac{(p^2 - M^2 - 2m_S^2)}{m_S^2}, \quad (15a)$$

$$f_2^{(1)}(p^2) = \frac{1}{2} \frac{|\phi^{(1)}(p^2)|^2}{(p^2 - m_Q^2)^2} \left(\frac{(m_Q^2 - M^2)}{m_S^2} (p^2 - M^2) + M^2 + 6Mm_Q - m_Q^2 - 2m_S^2 + 2p^2 \right). \quad (15b)$$

From Eqs.(3), (7) – (15) we can now calculate the quark distribution associated with process \mathcal{A} , which, because of the low mass present in the spectator state, should be a good approximation at large values of x .

B. Nucleon Structure Functions at Large x

At large x one can think of the photon scattering quasi-elastically from the constituent quark, in the sense that the internal structure of the CQ “quasi-particle” is not resolved. In this case the CQ structure function is a δ -function, and the resulting nucleon quark distribution given entirely by the momentum distributions $f_{Q/N}^{(S)}(y, p^2)$. Integrating $f_{Q/N}^{(S)}$ over p^2 gives then the valence quark distribution in the proton:

$$q_{\mathcal{A}}^{(S)}(x) = \int_x^1 \frac{dy}{y} \int_{-\infty}^{p_{max}^2(m_S^2, y)} dp^2 f_{Q/N}^{(S)}(y, p^2) \delta(1 - x_Q) = \int_{-\infty}^{p_{max}^2(m_S^2, y)} dp^2 f_{Q/N}^{(S)}(x, p^2), \quad (16)$$

where $x = Q^2/2P \cdot q$, $x_Q = x/y$ is the Bjorken variable of the CQ and the maximum value of the quark virtuality is given by Eq.(4).

The parameters defining the constituent quark distribution $f_{Q/N}^{(S)}$ (and hence $q_{\mathcal{A}}^{(S)}$) are as follows. Consistent with typical masses in effective constituent quark models, we take for the CQ mass $m_Q \approx 450$ MeV. For the scalar (pseudovector) diquark mass we use $m_{0(1)} \approx 1.0(1.2)$ GeV. These diquark masses are somewhat larger than in some model calculations of the nucleon’s static properties, which reflects the approximation that the low-mass spectator system can be described as a single diquark, Eq.(6). In fact, one would expect in effective CQ–diquark models to see a spectrum of diquark bound states with a range of masses [16]. By taking into account only the lightest diquark state one necessarily underestimates the average mass of the diquark which would effectively describe the low- s part of the spectrum. For comparison, we also examine the effect on the quark distributions of using smaller masses, $m_{0(1)} \approx 0.6(0.8)$ GeV.

For the QDN form factor (vertex function) specifying the distributions $f_{Q/N}^{(S=0,1)}$ we use the form in Eq.(13). The exponential parameters n_S in Eq.(13) are fixed by the behavior of the quark distribution at large x , since

$$p^2 \rightarrow -\frac{p_T^2}{(1-x)} \quad \text{as } x \rightarrow 1. \quad (17)$$

From Eqs.(17) and the expressions for $f_{Q/N}^{(S)}$ one finds that with $n_0 = 2.0$ and $n_1 = 3.5$ the quark distributions $q^{(0,1)}(x) \rightarrow (1-x)^{3,4}$ as $x \rightarrow 1$ [30]. The values of the cut-off parameters Λ_S in Eq.(13) are taken to be: $\Lambda_0 = 1.0$ GeV for the scalar vertex, and $\Lambda_1 = 1.2$ GeV for the $\gamma_5 \gamma_\alpha$ vertex.

Using these parameters, we show in Fig.4(a) the valence sum (solid curve), $x(u_V + d_V) \rightarrow 3x(q_A^{(0)} + q_A^{(1)})/2$, evolved from $\mu^2 = 1$ GeV² to $Q^2 = 10$ GeV². One sees that within the impulse approximation the valence quark distribution is almost a factor 2 larger than the data [30] (shaded) at $Q^2 = 10$ GeV². The position of the peak value of $x(u_V + d_V)$ depends quite sensitively on the mass of the intermediate state diquark system. For the smaller diquark masses ($m_{0(1)} = 0.6(0.8)$ GeV), the result (dashed) is nearly a factor 3 larger, and peaks at a considerably larger value of x compared with the data. The valence quark ratio in the impulse approximation, $d_V/u_V \rightarrow 2q_A^{(1)}/(3q_A^{(1)} + q_A^{(0)})$, shown in Fig.4(b), exhibits far less dependence on the diquark masses, and gives quite reasonable agreement with the data at large x , particularly for the larger mass spectators.

The fact that the impulse approximation is only good at large x is clearly reflected in the absence of the correct (singular) behavior of $q_A^{(S)}(x)$ as $x \rightarrow 0$ that would be expected from Regge phenomenology, namely $\sim x^{-\alpha_R}(\alpha_R \approx 1/2)$ (see Section IV.B). Because only small (finite) spectator masses are included in $q_A^{(S)}(x)$, the calculated distributions are finite at $x = 0$, whereas the experimental distributions diverge. Therefore a large fraction of the normalization has to come from the medium and large- x regions to compensate — hence the large peak in $x(u_V + d_V)$. This fact demonstrates that the distributions $q_A^{(S)}(x)$ alone, calculated in a CQ model, are incapable of describing the valence structure function over the entire range of x , and points to the necessity of including larger spectator masses,

corresponding to processes \mathcal{B} and \mathcal{C} outlined in Section II. In the next Section we describe the contributions to the structure functions from the larger spectator mass components of the quark spectral function.

IV. STRUCTURE OF CONSTITUENT QUARKS

As clearly seen in the previous Section, one should not expect valence quark distributions calculated from the handbag diagram alone to exhibit the correct behavior at small x . Since this is intrinsically related to the presence of low-mass spectators in the intermediate state, to rectify this deficiency one must consider in addition contributions to the spectral function ρ from states with masses larger than $m_S \sim M$.

A systematic formulation within the CQ picture developed in Section III is one in which the interactions among quarks are completely factored out of the basic QDN vertex. Interactions between quarks then give rise to effective constituent quark dressing — for process \mathcal{B} by a cloud of pions in the intermediate- s region, while for process \mathcal{C} by a soft “Reggeon cloud” at large s — which would result in CQs attaining substructure, Fig.2. The contribution from these processes to the quark distribution (direct photon diagram, Fig.2(a)) can then be written:

$$q_{\mathcal{B},\mathcal{C}}^{(S)}(x) = \int \frac{d^4 p}{(2\pi)^4} 2\pi \delta((P-p)^2 - m_S^2) \text{Tr} \left[\mathcal{Q}(p, q) \mathcal{H}^{(S)}(P, p) \right], \quad (18)$$

where the operator

$$\mathcal{Q}(p, q) = -i \int \frac{d^4 k}{(2\pi)^4} \delta((k+q)^2) \left[\not{q} (\not{k} - m_Q)^{-1} \mathcal{T}(p, k) (\not{k} - m_Q)^{-1} \right], \quad (19)$$

describes DIS from a dressed (generally off-shell) constituent quark. The trace in Eq.(18) is taken over the upper and lower quark indices in Fig.2(a). The crossed photon diagram in Fig.2(b) gives rise to an antiquark distribution $\bar{q}(x)$, which is given by an expression analogous to Eq.(19) with the substitution $q \rightarrow -q$.

The operator $\mathcal{T}(p, k)$ in Eq.(19) describes the truncated quark–quark interaction. In what follows we assume that \mathcal{T} is an analytic function of the invariant mass squared of

the quark-quark system, $s_Q = (p - k)^2$, of $u_Q = (p + k)^2$, and of the quark virtualities k^2 and p^2 . For real s_Q and u_Q , \mathcal{T} has a right-hand cut in the variable s_Q , a left-hand cut in u_Q , and singularities for $p^2 > 0$ and $k^2 > 0$. To make use of these properties in the loop integral in Eq.(19), it is convenient to parametrize the loop momentum k in terms of external momenta p and q : $k = \alpha p + \beta q' + k_T$, with $q' = x_Q p + q$, $x_Q = -q^2/2p \cdot q$ being the Bjorken variable of the CQ, and k_T is a two-dimensional vector perpendicular to both p and q . Then the δ -function in (19) fixes $\alpha = x_Q$. After integrating with respect to β , one finds that the operator \mathcal{Q} vanishes outside the interval $|x_Q| \leq 1$. For $0 \leq x_Q \leq 1$, \mathcal{Q} is given by a dispersion integral in s_Q along the right-hand (R) cut,

$$\mathcal{Q}_R(p, q) = \frac{1}{16\pi^3} \frac{1}{2p \cdot q} \int \frac{d^2 k_T ds_Q}{1 - x_Q} \frac{\text{Im}_R \not{q}(\not{k} + m_Q) \mathcal{T}(p, k)(\not{k} + m_Q)}{(k^2 - m_Q^2)^2}, \quad (20)$$

and hence contributes to the quark distribution. For $-1 \leq x_Q \leq 0$, the operator \mathcal{Q} is given by the dispersion integral along the (left-hand, L) cut in the u -channel,

$$\mathcal{Q}_L(p, q) = \frac{1}{16\pi^3} \frac{1}{2p \cdot q} \int \frac{d^2 k_T du_Q}{1 + x_Q} \frac{\text{Im}_L \not{q}(\not{k} + m_Q) \mathcal{T}(p, k)(\not{k} + m_Q)}{(k^2 - m_Q^2)^2}. \quad (21)$$

\mathcal{Q}_L determines in fact the contribution from the crossed photon diagram in the physical region $x_Q > 0$, and corresponds to the antiquark distribution in the CQ. To obtain the antiquark operator $\overline{\mathcal{Q}}$ from Eq.(21) one must substitute $q \rightarrow -q$ (and therefore $x_Q \rightarrow -x_Q$) and introduce an overall minus sign, $\overline{\mathcal{Q}}(p, q) = -\mathcal{Q}_L(p, -q)$ (see e.g. [9]).

Before discussing the details of the quark-quark interaction within our model, we can make one more model-independent observation about factorization of the total $\gamma^* N$ interaction. Let us firstly expand the operator \mathcal{Q} in terms of Dirac basis tensors:

$$\mathcal{Q}(p, q) = I \frac{\mathcal{Q}_0}{2m_Q} + \not{p} \frac{\mathcal{Q}_1}{2m_Q^2} + \not{q} \frac{\mathcal{Q}_2}{2p \cdot q}, \quad (22)$$

where the coefficients \mathcal{Q}_i ($i = 0, 1, 2$) scalar dimensionless functions of x_Q and p^2 . An expression similar to (22) holds for the antiquark operator with the scalar coefficients $\overline{\mathcal{Q}}_{0,1,2}$. Projecting \mathcal{Q} onto positive energy space and averaging over CQ spins one can define the quark and antiquark distributions in a CQ as:

$$q_Q(x_Q, p^2) = \frac{1}{2} \text{Tr} [(\not{p} + m_Q) \mathcal{Q}(p, q)] = \mathcal{Q}_0 + \frac{p^2}{m_Q^2} \mathcal{Q}_1 + \mathcal{Q}_2, \quad (23a)$$

$$\bar{q}_Q(x_Q, p^2) = \frac{1}{2} \text{Tr} [(\not{p} + m_Q) \bar{\mathcal{Q}}(p, q)] = \bar{\mathcal{Q}}_0 + \frac{p^2}{m_Q^2} \bar{\mathcal{Q}}_1 + \bar{\mathcal{Q}}_2. \quad (23b)$$

For a quark (antiquark) with no internal structure one can easily show that in the Bjorken limit only a single function is non-zero: $\mathcal{Q}_2 \neq 0$ ($\bar{\mathcal{Q}}_2 \neq 0$), while $\mathcal{Q}_{0,1} = 0$ ($\bar{\mathcal{Q}}_{0,1} = 0$). On the other hand, for a constituent quark with internal structure all three coefficients can be non-zero and therefore contribute to the quark (antiquark) distribution.

Finally, substituting (22) into Eq.(18) and using Eqs.(9), (10) and (23a), the contribution to the nucleon's quark distribution from dressed CQs is:

$$q_{\mathcal{B},c}^{(S)}(x) = \int_x^1 \frac{dy}{y} \int^{p_{max}^2(m_S^2, y)} dp^2 \left[f_{Q/N}^{(S)}(y, p^2) q_Q \left(\frac{x}{y}, p^2 \right) + \Delta f_0^{(S)}(y, p^2) \mathcal{Q}_0 \left(\frac{x}{y}, p^2 \right) + \Delta f_1^{(S)}(y, p^2) \mathcal{Q}_1 \left(\frac{x}{y}, p^2 \right) \right], \quad (24)$$

where $f_{Q/N}^{(S)}(y, p^2)$ is given by (10) while the functions $\Delta f_{0,1}^{(S)}$ are

$$\Delta f_0^{(S)}(y, p^2) = \frac{y}{32\pi^2 m_Q} \text{Tr} [\mathcal{H}^{(S)}(P, p)] - f_{Q/N}^{(S)}(y, p^2), \quad (25a)$$

$$\Delta f_1^{(S)}(y, p^2) = \frac{y P \cdot p - p^2}{8\pi^2 m_Q^2} f_1^{(S)}(p^2). \quad (25b)$$

A similar expression can be written for the antiquark distribution $\bar{q}(x)$ with the substitution $\mathcal{Q}_i \rightarrow \bar{\mathcal{Q}}_i$ and $q_Q \rightarrow \bar{q}_Q$.

The first term in Eq.(24) is a generalization of Eq.(16) for an ‘undressed’ CQ to the case of a CQ having non-trivial internal structure, and is written as a convolution of the CQ distribution $f_{Q/N}^{(S)}$ and the spin averaged CQ structure function q_Q , Eq.(23a). One sees, however, that the non-trivial Dirac structure of the $\gamma^* Q$ interaction leads to the convolution breaking terms in Eq.(24) which thus render the convolution hypothesis [13,44,36] invalid. Note also that a simple convolution formulation of the structure functions is recovered in the $p^2 \rightarrow m_Q^2$ limit, since the terms $\Delta f_{0,1}$ come with an extra factor of $(p^2 - m_Q^2)$ compared with the $f_{Q/N}^{(S)}$ term.

As discussed in Section II, it is convenient to split the spectrum of invariant masses of the quark–quark system into two regions: small s_Q ($s_Q < M^2$) and large s_Q ($s_Q > M^2$). In

what follows we consider a model where the interaction \mathcal{T} is described by meson exchanges for the low-mass region, while to evaluate the effect from the large-mass region we adopt a simple model based on Regge phenomenology.

A. Pion-Dressed Constituent Quarks (Process \mathcal{B})

In evaluating the effect of the dressing of CQs by meson “clouds”, we will restrict ourselves to pions. Contributions from CQs dressed by higher mass mesons (e.g. ρ, ω , etc.) will be largely suppressed by the larger meson masses [34], and only ever become noticeable when unrealistically hard form factors are employed. In addition, predictions for the ρ and heavier mesons are less reliable in constituent quark models due to threshold effects, if one uses CQ masses of the order ~ 400 MeV.

For the interaction of CQs with pions we will utilize the simple effective chiral Lagrangian, valid at scales below ~ 1 GeV, similar to that considered in Refs. [35,36], in which the leading interaction is given by:

$$\mathcal{L}_{Q\pi} = -\frac{g_A}{\sqrt{2}f_\pi} \bar{\psi}_Q \gamma^\alpha \gamma_5 \psi_Q \partial_\alpha \phi_\pi. \quad (26)$$

Here ψ_Q and ϕ_π are the CQ and pion fields, $g_A \approx 0.75$ is the axial coupling constant of the constituent quark, and $f_\pi = 93$ MeV is the pion decay constant. A typical process which arises from this interaction Lagrangian is depicted in Fig.5. Note that the pion fields appearing in $\mathcal{L}_{Q\pi}$ represent point-like pions. In principle $\mathcal{L}_{Q\pi}$ gives rise therefore also to terms involving the direct coupling of photons to pions. At high energies, however, the pion’s substructure would be expected to play a role, and these contributions, through the presence of the pion form factor, would be suppressed. Furthermore, the direct $\gamma^*\pi$ couplings would also violate the Callan-Gross relation, and as such they are not considered.

In the present work we consider only order $\mathcal{O}(1/f_\pi)$ effects from $\mathcal{L}_{Q\pi}$. The relevant process to be considered is therefore the one-pion exchange process in Fig.6 (together with the crossed photon diagram). Note that scattering from the pion cloud itself, as would be

needed to generate antiquark distributions, for example, would enter only at order $\mathcal{O}(1/f_\pi)^2$ from the Lagrangian [37]. The pion cloud contributions were considered in Ref. [36], however, the expansion of $\mathcal{L}_{Q\pi}$ was performed only up to $\mathcal{O}(1/f_\pi)$.

The quark-quark operator \mathcal{T} for the one pion exchange interaction can then be obtained from (26) by a Fierz transformation:

$$\text{Im}_R \mathcal{T}^\pi = 2\pi\delta\left((p-k)^2 - m_\pi^2\right) \mathcal{F}\left(\Gamma^\pi \bar{\Gamma}^\pi\right), \quad (27)$$

where $\Gamma^\pi = (g_A/\sqrt{2}f_\pi)(\not{p} - \not{k})\gamma_5\phi_{Q\pi}$ represents the $QQ\pi$ vertex, with $\phi_{Q\pi}$ being the $QQ\pi$ vertex function, and \mathcal{F} is the Fierz transformation operator. Substituting (27) into (20), we find the one pion exchange contribution to the coefficient functions \mathcal{Q}_i :

$$\mathcal{Q}_0^\pi = \frac{1}{8\pi^2} \left(\frac{g_A m_Q}{\sqrt{2}f_\pi}\right)^2 \int_{-\infty}^{k_{max}^2} dk^2 \frac{\phi_{Q\pi}^2}{(k^2 - m_Q^2)^2} \{-x_Q m_\pi^2\}, \quad (28a)$$

$$\begin{aligned} \mathcal{Q}_1^\pi &= \frac{1}{8\pi^2} \left(\frac{g_A m_Q}{\sqrt{2}f_\pi}\right)^2 \int_{-\infty}^{k_{max}^2} dk^2 \frac{\phi_{Q\pi}^2}{(k^2 - m_Q^2)^2} \\ &\times \left\{ (1 - x_Q) (m_Q^2 - k^2 + x_Q(p^2 - m_Q^2)) - x_Q m_\pi^2 \right\}, \end{aligned} \quad (28b)$$

$$\begin{aligned} \mathcal{Q}_2^\pi &= \frac{1}{8\pi^2} \left(\frac{g_A m_Q}{\sqrt{2}f_\pi}\right)^2 \int_{-\infty}^{k_{max}^2} dk^2 \frac{\phi_{Q\pi}^2}{(k^2 - m_Q^2)^2} \frac{1}{m_Q^2} \\ &\times \left\{ (p^2(2x_Q - 1) - k^2) (m_Q^2 - k^2 + x_Q(p^2 - m_Q^2)) + x_Q m_\pi^2 (p^2 - m_Q^2) \right\}. \end{aligned} \quad (28c)$$

The kinematical maximum of the quark virtuality, $k_{max}^2(s_Q, x_Q, p^2)$, is given by Eq.(4), with $s_Q = m_\pi^2$ and the nucleon mass squared M^2 replaced by p^2 .

Equations (28) determine the pion contribution to the quark distribution in the CQ via Eq.(24). Similar expressions arise for the pion contribution to the antiquark distribution, $\overline{\mathcal{Q}}_i^\pi$, and are related to (28) by crossing symmetry, viz. interchanging $x_Q \rightarrow -x_Q$ and introducing an overall minus sign. In the present work we consider the pion contribution to the valence part of the nucleon quark distribution, so that only terms even in x_Q survive. In this case the scalar term \mathcal{Q}_0^π cancels out and the convolution breaking term in Eq.(24) arises only from the Dirac structure \not{p} in Eq.(22).

In Eqs.(28) the integral over k^2 is regularized by a sharp cut-off, $\Lambda_{Q\pi}$, whereby the $QQ\pi$ vertex function is parametrized by a theta-function:

$$\phi_{Q\pi}(k^2, p^2) = \Theta(k^2 + \Lambda_{Q\pi}^2) \Theta(p^2 + \Lambda_{Q\pi}^2), \quad (29)$$

where we have also parametrized the p^2 dependence of this vertex by a similar cut-off (for other forms of the cut-off see Refs. [36,38,39]). The parameter $\Lambda_{Q\pi}$ represents a typical scale beyond which the effective interaction in Eq.(26) is no longer a valid approximation to QCD, and is usually taken to be of the order $\Lambda_{Q\pi} \sim 1$ GeV [35].

In Fig.7 we plot the one-pion exchange contribution to the sum of the valence $u_V \left(\rightarrow 3/2 \left(q_B^{(0)} - \bar{q}_B^{(0)} \right) + 5/2 \left(q_B^{(1)} - \bar{q}_B^{(0)} \right) \right)$ and $d_V \left(\rightarrow 3 \left(q_B^{(0)} - \bar{q}_B^{(0)} \right) + 2 \left(q_B^{(1)} - \bar{q}_B^{(1)} \right) \right)$ distributions, compared with the impulse approximation contribution, for three values of the ultra-violet cut-off $\Lambda_{Q\pi}$, namely 0.8, 1.0 and 1.2 GeV. The results indicate that for reasonable values of $\Lambda_{Q\pi}$ ($\lesssim 1$ GeV), the one-pion exchange contribution is certainly not negligible for $x \lesssim 0.2$, and indeed provides around 15-20% of the valence quark normalization compared to the impulse approximation distributions associated with process \mathcal{A} . (Similar numbers are obtained in non-covariant, infinite momentum frame calculations, where one makes use of a transverse momentum cut-off, $\phi_{Q\pi} = \Theta(k_T^2 - \Lambda_{Q\pi}^2)$ — see Appendix A.) However, it is also apparent that DIS from dressed CQ is not able to provide sufficiently soft contributions to the nucleon quark distribution that would simulate Regge behavior. Agreement with large Q^2 DIS data would still require evolution from scales similar to that needed for process \mathcal{A} alone, $\mu^2 \sim 0.2$ GeV² [23]. Adding higher order contributions would make the total distribution softer, however, one would need to include quite high orders to come close to reproducing the required degree of singularity as $x \rightarrow 0$. The complexity involved in performing even the 2-loop calculation [37] based on the effective interaction $\mathcal{L}_{Q\pi}$ is quite daunting! In the next Section we shall examine a more efficient method of incorporating the larger mass continuum of spectator states (above $s \sim 2$ GeV²), based on Regge phenomenology.

B. Asymptotic Spectator Masses (Process \mathcal{C})

It should be clear by now that to obtain quark distributions which are sufficiently soft at small x to be compatible with DIS data (when evolved from our model scale of $\mu^2 \sim 1 \text{ GeV}^2$) one must include contributions to the spectator spectral function from the large-mass continuum. As mentioned earlier (see also Ref. [9]), the physical mechanism to which one can attribute the large mass states is the high-energy scattering of the $q\bar{q}$ components of the photon from the nucleon. By examining the structure of the energy denominators of the $q\bar{q} + N$ system in the target rest frame one can immediately see that this time-ordering dominates the contribution from the direct scattering of the photon from a quark in the target. The virtual $q\bar{q}$ fluctuation excites the target into states with a spectrum of masses $s \gtrsim \mathcal{O}(M^2)$.

In modeling the large- s contribution to the spectral function it will be convenient to make use of well-known ideas from the Regge poles approach to high-energy scattering [3]. Formally, the sum over the spectator masses s can be shown to be effectively described by the exchange of Regge trajectories in the complex angular momentum plane. In a constituent quark model, where the interaction of the photon with the CQ is factored from the total amplitude, the $q\bar{q}$ pair will in fact excite the CQ in the nucleon, which necessitates integrating over states that are spectator to the γ^*Q collision. The problem then reduces to describing the asymptotic behavior of the quark–quark interaction $\mathcal{T}(p, k)$ in terms of exchange of Regge poles, Fig.3(c) (for an alternative description of high-energy quark–quark scattering see Ref. [41].)

The leading contribution to the asymptotic scattering amplitude comes from the Pomeron exchange, which, however, cancels out in the valence quark distribution. The relevant Regge trajectories therefore correspond to the exchange of vector mesons, and we will assume that the corresponding Reggeons couple to quarks like vector mesons. In this case the quark–quark scattering amplitude at high energies can be written:

$$\mathcal{T}(p, k) = \gamma_{(q)\mu} \gamma_{(Q)}^\mu \frac{T(s_Q, u_Q; k^2, p^2)}{s_Q - u_Q}, \quad (30)$$

where T is a Lorentz-invariant function, whose interpretation becomes clear if we project \mathcal{T} onto positive energy space and average over quark spins:

$$T(s_Q, u_Q; k^2, p^2) = \frac{1}{4} \text{Tr}_q \text{Tr}_Q [(-\not{k} + m_Q)(\not{p} + m_Q) \mathcal{T}(p, k)]. \quad (31)$$

Here the trace is taken over the upper and lower quark indices in Fig.2, which we distinguish by indices (q) and (Q) , respectively. Therefore the function $T(s_Q, u_Q; k^2, p^2)$ can be considered as an analytical continuation of the spin-averaged quark-quark scattering amplitude into the off-mass-shell region. In general T describes both the qQ and $\bar{q}Q$ scattering channels, which are connected by crossing symmetry. Namely, in the s -channel $T(s_Q, u_Q; k^2, p^2)$ coincides with the $\bar{q}Q$ scattering amplitude, $T_{\bar{q}Q}(s_Q; k^2, p^2)$, which contributes to the quark distribution, while in the u -channel it is identified with the qQ amplitude, $T_{qQ}(u_Q; k^2, p^2)$, from which one obtains the antiquark distribution.

For the interaction (30), the coefficients $\mathcal{Q}_{0,1,2}^R$ in the high-energy (Regge) region become:

$$\mathcal{Q}_0^R = 0, \quad (32a)$$

$$\mathcal{Q}_1^R = \frac{1}{(2\pi)^3} \int ds_Q \int_{-\infty}^{k_{max}^2} dk^2 \frac{\text{Im} T_{\bar{q}Q}(s_Q; k^2, p^2)}{(k^2 - m_Q^2)^2} \left\{ \frac{2m_Q^2 x_Q^2}{s_Q - p^2 - k^2} \right\}, \quad (32b)$$

$$\mathcal{Q}_2^R = \frac{1}{(2\pi)^3} \int ds_Q \int_{-\infty}^{k_{max}^2} dk^2 \frac{\text{Im} T_{\bar{q}Q}(s_Q; k^2, p^2)}{(k^2 - m_Q^2)^2} \left\{ -x_Q + \frac{m_Q^2 - k^2 - 2x_Q^2 p^2}{s_Q - p^2 - k^2} \right\}, \quad (32c)$$

where $k_{max}^2 = k_{max}^2(s_Q, x_Q, p^2)$ is given by Eq.(4), with the nucleon mass squared M^2 replaced by p^2 . Together with Eq.(24), these give the contribution to the nucleon quark distribution from the $q\bar{q}$ scattering mechanism. Expressions for the antiquark distributions, $\overline{\mathcal{Q}}_{0,1,2}^R$, can be obtained by applying the crossing symmetry rules. The final result is similar to Eqs.(32), with the $\bar{q}Q$ scattering amplitude $T_{\bar{q}Q}$ replaced by the qQ scattering amplitude T_{qQ} .

To finally calculate the Regge-exchange contribution to the quark (q_c) and antiquark (\bar{q}_c) distributions from Eqs.(24,32) requires modeling the $\bar{q}Q$ and qQ scattering amplitudes.

As discussed in Ref. [9], at high energy and low x one can approximate $T_{\bar{q}Q}$ and T_{qQ} by the constituent quark–target amplitudes obtained from the simple additive quark model of high-energy hadron scattering. In this case, the nucleon–nucleon scattering amplitude can be expressed in terms of the quark–quark amplitude and the CQ distribution functions $f_{Q/N}$:

$$\frac{T_{NN'}(s_N)}{s_N} = \int [dp] [dp'] f_{Q/N}(y, p^2) f_{Q/N}(y', p'^2) \frac{T_{QQ'}(s_Q, p^2, p'^2)}{s_Q} \quad (33)$$

where s_N is now the total hadronic center of mass energy squared, p and p' are the four-momenta of CQs in nucleons N and N' , with y and y' the light-cone momentum fractions carried by quarks Q and Q' , and $s_Q = (p+p')^2$ is the invariant mass squared of the interacting QQ' system. The brackets in Eq.(33) denote: $\int [dp] \equiv \int_0^1 dy/y \int_{-\infty}^{p_{max}(m_s^2, y)} dp^2$. At high energy, where $s_Q \approx y y' s_N$, one can obtain approximate solutions to Eq.(33) by evaluating the quark–quark amplitude at averaged values of y and p^2 [9]. With the QDN vertex model parameters in Section III, one finds $\langle y \rangle \sim 1/3$ and $\langle p^2 \rangle \sim -(0.3 - 0.4) \text{ GeV}^2$.

The s_Q -dependence of the amplitudes corresponding to the valence quark distribution, namely the difference $\Delta T_{QQ} \equiv T_{\bar{q}Q} - T_{qQ}$, is then fixed directly by the energy dependence of the $\bar{p}p$ and pp amplitude difference. In the Regge approach this difference is determined by the exchange of the spin-1 ω -meson trajectory:

$$\text{Im}(T_{\bar{p}p}(s_N) - T_{pp}(s_N)) = s_N^{\alpha_\omega} R_\omega, \quad (34)$$

where R_ω is the residue of the ω Reggeon trajectory, and α_ω the intercept. The best fit of Ref. [42] gives $R_\omega \approx 42 \text{ mb} \cdot \text{GeV}^{1-\alpha_\omega}$ and $\alpha_\omega = 0.548$. For the p^2 and k^2 dependence of ΔT_{QQ} we follow Ref. [9] in adopting the following factorized form:

$$\Delta T_{QQ}(s_Q; k^2, p^2) = g_R(k^2) g_R(p^2) \Delta T_{QQ}(s_Q; 0, 0), \quad (35)$$

where the form factor functions g_R describe the fall-off with four-momentum of the total quark–quark amplitude:

$$g_R(p^2) = \left(1 - p^2/\Lambda_R^2\right)^{-n_R}. \quad (36)$$

For the exponent n_R we choose the value $n_R \approx 4$ to correctly reproduce the tail of the resulting distribution function at large x , while the cut-off Λ_R remains a free parameter, to be determined by fitting to the DIS data. The best fit to the data gives $\Lambda_R \approx 0.25$ GeV.

Finally, with these ingredients the contributions to the u_V and d_V valence quark distributions from process \mathcal{C} are both given by $3/2 \left((q_C^{(0)} - \bar{q}_C^{(0)}) + (q_C^{(1)} - \bar{q}_C^{(1)}) \right)$, where $q_C^{(0,1)}$ are obtained from Eqs.(24), (25) and (32).

V. RESULTS AND CONCLUSIONS

With the inclusion of all three processes \mathcal{A} , \mathcal{B} and \mathcal{C} , describing the low, intermediate and high-mass spectrum of spectator states, respectively, the valence u and d quark distribution are given by:

$$u_V(x) = Z_u \{ u_{\mathcal{A}}(x) + (u_{\mathcal{B}}(x) - \bar{u}_{\mathcal{B}}(x)) + (u_{\mathcal{C}}(x) - \bar{u}_{\mathcal{C}}(x)) \}, \quad (37a)$$

$$d_V(x) = Z_d \{ d_{\mathcal{A}}(x) + (d_{\mathcal{B}}(x) - \bar{d}_{\mathcal{B}}(x)) + (d_{\mathcal{C}}(x) - \bar{d}_{\mathcal{C}}(x)) \}. \quad (37b)$$

The normalization constants $Z_{u,d}$ are determined by charge conservation,

$$Z_u = \frac{2}{2 + \langle u - \bar{u} \rangle_{\mathcal{B}} + \langle u - \bar{u} \rangle_{\mathcal{C}}}, \quad (38a)$$

$$Z_d = \frac{1}{1 + \langle d - \bar{d} \rangle_{\mathcal{B}} + \langle d - \bar{d} \rangle_{\mathcal{C}}}, \quad (38b)$$

where the brackets $\langle \dots \rangle$ denote the first moment, and where the impulse approximation contributions, $d_{\mathcal{A}}$ and $u_{\mathcal{A}}$ are normalized to 1 and 2, respectively.

The relative normalizations of the individual contributions from $\mathcal{A} - \mathcal{C}$ are completely fixed in terms of the parameters described in Sections III and IV. The contributions to the normalization of the valence $u_V + d_V$ distribution from one pion exchange is $\approx 16\%$, while the Regge exchange contribution is $\approx 28\%$. This means that the impulse approximation contribution (process \mathcal{A}) is renormalized by $Z_u = 62\%$ and $Z_d = 43\%$ for the u and d distributions, respectively, and contributes about 56% to the total normalization. The contributions to the second moments of $u_V + d_V$ at the input scale are $\approx 41\%$, 6% and 0.06%,

so that some 53% of the nucleon's momentum at $\mu^2 = 1 \text{ GeV}^2$ is left to be carried by sea quarks and gluons.

The results for $x(u_V + d_V)$, evolved from $\mu^2 = 1 \text{ GeV}^2$, are plotted in Fig.8, in comparison with the data (shaded) at $Q^2 = 10 \text{ GeV}^2$. Also shown for comparison are the corresponding results for processes \mathcal{A} and \mathcal{B} , and \mathcal{A} alone. In total, the results indicate that one can indeed obtain a good description of data above $\mu^2 = 1 \text{ GeV}^2$ in terms of CQ parameters. This scale, being at the boundary of the scales which are generally accepted as reliable for perturbative evolution, is considerably larger than those used in many previous attempts to calculate leading twist quark distributions (which typically have needed $\mu^2 \sim 0.1 - 0.3 \text{ GeV}^2$). This is one of the main results of the present work.

As possible extensions of this work, one could next attempt to incorporate sea quark distributions into the formalism at small x , which would require a more detailed analysis of processes \mathcal{B} and \mathcal{C} . In the former, the sea would simply be associated with the antiquark content of the pion cloud. However, to adequately describe the low- x region one would need to extend the Reggeon model for process \mathcal{C} to include in addition the exchange of Pomeron trajectories between quarks. Another possible test of the model would be to consider polarization observables, such as the nucleon's spin-dependent g_1 structure function.

Finally, we should state that while our formalism is quite general, it is nevertheless a formidable challenge to embed within any specific model the full spectator mass spectrum, so as to describe consistently the nucleon's structure function over the whole range of Bjorken- x . Our attempt here to obtain such a unified description suggests, however, that constituent quarks may still be the most relevant degrees of freedom appropriate for this task, and for the more general problem of understanding the nucleon's non-perturbative structure in DIS.

ACKNOWLEDGMENTS

We would like to thank H.Forkel, G.Piller, C.M.Shakin and C.Stangl for useful comments and discussions. This work was supported by the BMBF.

APPENDIX A: CONSTITUENT QUARKS IN THE INFINITE MOMENTUM FRAME

In this Appendix we discuss an alternative, non-covariant, formulation of DIS from constituent quarks to that in Section IV. In a covariant formalism contributions to the quark distribution functions from DIS off dressed CQs can be expressed as a two-dimensional convolution (in y and p^2) of the CQ distribution $f_{Q/N}$ and the off-shell CQ structure function q_Q , plus a non-convolution term whose contribution is proportional to $(p^2 - m_Q^2)$. In the on-mass-shell limit this term would vanish, leaving only the convolution term. Furthermore, the remaining term would reduce to a one-dimensional convolution in the momentum fraction y only. From a practical point of view, this would considerably reduce the number of integrations needed, and simplify calculations involving higher-order, multi-loop, pion-dressing contributions.

A framework in which one-dimensional convolution equations can be recovered is non-covariant time-ordered perturbation theory in the infinite momentum frame (IMF). Because here all particles are on-mass-shell, the non-convolution off-shell corrections in Eqs.(24) are identically zero, and factorization of subprocesses is automatic. Furthermore, in the IMF the so-called Z -diagrams, which involve antiparticles, or particles moving backwards in time, are suppressed by powers of $1/P_L$ [32], where P_L is the longitudinal momentum of the target. Hence only forward moving particles are ever considered. It is only within this approach that one can consider the function $f_{Q/N}$ (integrated over transverse momentum) as a genuine probability distribution function — in any other frame one must also incorporate antiquark components into the virtual constituent quark (the IMF is also the most appropriate context in which to view the $q \rightarrow q\pi$ splitting functions of Eichten et al. [36,44], and the nucleon \rightarrow nucleon + π distributions of Refs. [33,34].) Therefore the simple one-dimensional convolution formulation is necessarily frame-dependent.

By way of illustration, let us examine the one-pion exchange contribution to the quark distribution function, as in Fig.6, in the IMF. The momentum of a nucleon moving with

longitudinal momentum P_L in the IMF can be parametrized as [32,33]:

$$P_\mu = \left(P_L + \frac{M^2}{2P_L}; \mathbf{0}_T, P_L \right). \quad (\text{A1a})$$

Similarly for the CQ and spectator diquark momenta, we have:

$$p_\mu = \left(|y|P_L + \frac{m_Q^2 + p_T^2}{2|y|P_L}; \mathbf{p}_T, yP_L \right), \quad (\text{A1b})$$

$$p'_\mu = \left(|1-y|P_L + \frac{m_S^2 + p_T^2}{2|1-y|P_L}; -\mathbf{p}_T, (1-y)P_L \right), \quad (\text{A1c})$$

and for the struck quark and spectator pion:

$$k_\mu = \left(|x|P_L + \frac{m_Q^2 + \left(\mathbf{k}_T + \frac{x}{y}\mathbf{p}_T\right)^2}{2|x|P_L}; \mathbf{k}_T + \frac{x}{y}\mathbf{p}_T, xP_L \right), \quad (\text{A1d})$$

$$k'_\mu = \left(|y-x|P_L + \frac{m_\pi^2 + \left(-\mathbf{k}_T + \left(1 - \frac{x}{y}\right)\mathbf{p}_T\right)^2}{2|y-x|P_L}; \right. \\ \left. -\mathbf{k}_T + \left(1 - \frac{x}{y}\right)\mathbf{p}_T, (y-x)P_L \right), \quad (\text{A1e})$$

respectively. Evaluating the trace as in Eq.(19) in terms of these momenta, one finds the contribution to the valence quark distribution from a constituent quark dressed by a pion:

$$q_B^{(S)}(x) = \int_x^1 \frac{dy}{y} \int_0^\infty dp_T^2 f_{Q/N}^{(S)}(y, p_T) \int_0^\infty dk_T^2 q_{Q\pi/Q}(x_Q, k_T), \quad (\text{A2})$$

where in the IMF the functions $f_{Q/N}^{(S)}$ are given by:

$$f_{Q/N}^{(0)}(y, p_T) = \frac{1}{16\pi^2} \frac{|\phi^{(0)}(y, p_T)|^2}{y^2 (M^2 - M_{QD}^2)^2} \left\{ p_T^2 + (m_Q + yM)^2 \right\} \quad (\text{A3})$$

for $S = 0$ spectators, and

$$f_{Q/N}^{(1)}(y, p_T) = \frac{1}{16\pi^2} \frac{|\phi^{(1)}(y, p_T)|^2}{y (M^2 - M_{QD}^2)^2} \left\{ 6Mm_Q + 2P \cdot p + \frac{4P \cdot p' p \cdot p'}{m_S^2} \right\} \quad (\text{A4})$$

for $S = 1$ intermediate states. The variable

$$M_{QD}^2 \equiv (p + p')^2 = \frac{m_Q^2 + p_T^2}{y} + \frac{m_S^2 + p_T^2}{1-y} \quad (\text{A5})$$

is the squared mass of the virtual quark-spectator diquark system. Note that the IMF expressions for $f_{Q/N}^{(S)}(y, p_T)$ can be related to the covariant expressions in Section III (apart from the QDN vertex function) if one observes that p_μ in Eq.(A1b) satisfies:

$$p_\mu p^\mu = -\frac{p_T^2}{1-y} + p_{max}^2, \quad (\text{A6})$$

where p_{max}^2 is given by Eq.(4).

The function:

$$q_{Q\pi/Q}(x_Q, k_T) = \frac{1}{8\pi^2} \left(\frac{g_A m_Q}{\sqrt{2} f_\pi} \right)^2 \frac{|\phi_{Q\pi}(x_Q, k_T)|^2}{x_Q^2 (1-x_Q) (m_Q^2 - M_{Q\pi}^2)^2} \{k_T^2 + m_Q^2 (1-x_Q)^2\} \quad (\text{A7})$$

represents the (unintegrated) structure function of a CQ dressed by a pion (see Eqs.(23a), (28)), where the squared mass of the $Q\pi$ state is given by:

$$M_{Q\pi}^2 \equiv (k + k')^2 = \frac{m_Q^2 + k_T^2}{x_Q} + \frac{m_\pi^2 + k_T^2}{1-x_Q}. \quad (\text{A8})$$

One can easily demonstrate that a pseudoscalar $Q\pi$ interaction leads to the same result as in Eq.(A7), by virtue of the IMF on-mass-shell condition for the CQs (i.e. $p_\mu p^\mu = m_Q^2$ in Eq.(28)), and the Goldberger-Treiman relation [16].

Although the kinematical (or trace) factors are similar in the covariant and IMF calculations, the connection between the vertex functions (or form factors) in the two approaches is not a straightforward one. Covariantly, the vertex function such as in Eq.(13) can only depend on the virtuality of the exchanged off-mass-shell particle, p^2 . In the time-ordered IMF approach the vertex function cannot depend on the p^2 , but rather must be a function of the variable M_{QD}^2 . This constraint stems from the requirement that the momentum distribution functions respect probability and momentum conservation, hence must display explicit symmetry under the interchange $y \leftrightarrow 1-y$ (Eq.(B1) in Appendix B below), which cannot be the case in a covariant formulation.

Since the p_T and k_T dependence in Eq.(A2) is factorized, one can write the total quark distribution as a one-dimensional convolution of the CQ structure function, q_Q , with the p_T -integrated CQ distribution $f_{Q/N}^{(S)}$ (c.f. Eq.(24)):

$$q_B^{(S)}(x) = \int_x^1 \frac{dy}{y} \tilde{f}_{Q/N}^{(S)}(y) q_Q\left(\frac{x}{y}\right), \quad (\text{A9})$$

where

$$\tilde{f}_{Q/N}^{(S)}(y) = \int dp_T^2 f_{Q/N}^{(S)}(y, p_T), \quad (\text{A10})$$

and

$$q_Q(x_Q) = \int dk_T^2 q_{Q\pi/Q}(x_Q, k_T). \quad (\text{A11})$$

The convolution formula (A9) can also be easily generalized to the case of n pions in the intermediate state, as in Fig.3(b):

$$q_{(n)}^{\pi(S)} = \int \frac{dy_1}{y_1} \cdots \frac{dy_n}{y_n} \tilde{f}_{Q/N}^{(S)}(y_1) q_Q(y_2/y_1) \cdots q_Q(y_n/y_{n-1}) q_Q(x/y_n). \quad (\text{A12})$$

As mentioned above, a formulation of the higher-order diagrams in terms of simple convolution integrals enables fewer integrations over coupled momenta to be performed, which simplifies considerably the numerical evaluation of these contributions.

APPENDIX B: DIQUARK STRUCTURE

In this Appendix we discuss DIS from possible diquark constituents in the nucleon. If one takes seriously the quark–diquark picture of the nucleon, in which the diquark itself is treated as an effective quasi-particle, then one must also consider the process where a diquark is struck by the DIS probe, Fig.9, which then requires modeling the structure function of a bound diquark. (Although any realistic model of the nucleon, which is to reproduce the Callan-Gross relation, cannot have diquarks as elementary constituents.) For scalar diquarks this process was considered by Suzuki et al. [14]. In a covariant framework scattering from $S = 1$ diquarks is more problematic, however, as was demonstrated in Ref. [34] for DIS off spin-1 meson configurations in the nucleon. Within the IMF approach discussed in Appendix A above, calculating the diquark distribution is considerably simpler — in fact one expects explicit symmetry between the constituent quark and diquark distribution functions:

$$f_{D/N}^{(S)}(y) = f_{Q/N}^{(S)}(1 - y), \quad (\text{B1})$$

where $f_{D/N}^{(S)}(y)$ is the probability distribution of spin S diquarks in the nucleon with momentum fraction y . In a covariant treatment this symmetry, which is ‘screened’ by off-mass-shell effects, need not be explicit.

The relation in Eq.(B1) is readily obtained from any QDN vertex function that is a function of the variable $M_{QD}^2 \equiv (m_Q^2 + p_T^2)/y + (m_S^2 + p_T^2)/(1 - y)$ (see Eq.(A5)) — for example a multipole form: $\phi^{(S)} \propto 1/(\Lambda_S^2 + M_{QD}^2)^{n_S}$. With the interchange of $m_Q \leftrightarrow m_S$ and $y \leftrightarrow 1 - y$, this choice automatically results in the relation (B1) [23,34,40]. This constraint on the CQ–diquark symmetry consequently imposes constraints upon the shape of the quark distribution. Phenomenologically, the main difference between these forms arises at small x , where the M_{QD}^2 -dependent functions give somewhat smaller distributions. The reason for this is the $1/y$ factor in M_{QD}^2 , which at small x serves to suppress the quark distributions, which themselves depend on inverse powers of M_{QD}^2 .

Having outlined how one could systematically include DIS contributions from diquarks, we should point out however that DIS from diquarks is in fact a next-to-leading order process in the QQ coupling constant G . Hence it should be treated on the same footing as the order $(1/f_\pi)^2$ processes involving pion dressing, such as the direct scattering from the nucleon’s pion cloud. While the higher-order (higher-mass) processes can in principle be systematically included, it is in fact more efficient to describe them in terms of the Regge model described in Section IV.B.

REFERENCES

- [1] H1 Collaboration, Nucl.Phys. B 407 (1993) 515; ZEUS Collaboration, Phys.Lett. B 316 (1993) 412; S.Keller, et al., Phys.Lett. B 270 (1991) 61; L.H.Orr and W.J.Stirling, Phys.Rev.Lett. 66 (1991) 1673; W.-K.Tang, Phys.Lett. B 278 (1992) 363; A.J.Askew, et al., Phys.Lett. B 325 (1994) 212; A.J.Askew, J.Kwiecinski, A.D.Martin and P.J.Sutton, Phys.Rev. D 49 (1994) 4402; J.R.Forshaw, P.N.Harriman and P.J.Sutton, Nucl.Phys. B 416 (1994) 739; K.Golec-Biernat, M.W.Krasny and S. Riess, Phys.Lett. B 337 (1994) 367.
- [2] R.L.Jaffe, Phys.Rev. D 11 (1975) 1953; R.L.Jaffe and G.G.Ross, Phys.Lett. B 93 (1980) 313; L.S.Celenza and C.M.Shakin, Phys.Rev. C 27 (1983) 1561; C.J.Benesh and G.A.Miller, Phys.Rev. D 36 (1987) 1344; A.W.Schreiber, A.W.Thomas and J.T.Londergan, Phys.Rev. D 42 (1990) 2226; A.W.Schreiber, P.J.Mulders, A.I.Signal and A.W.Thomas, Phys.Rev. D 45 (1992) 3069; M.Traini, L.Conci and U.Moschella, Nucl.Phys. A 544 (1992) 731; F.M.Steffens and A.W.Thomas, Nucl.Phys. A 568 (1992) 798; C.J.Benesh, T.Goldman and G.J.Stephenson, Jr., Phys.Rev. C 48 (1993) 1379; H.J.Weber, Phys.Rev. D 49 (1994) 3160.
- [3] P.D.B.Collins, *Regge Theory and High Energy Physics* (Cambridge University Press, Cambridge, 1977).
- [4] M.Glück, E.Reya and A.Vogt, Z.Phys. C 48 (1990) 471; Z.Phys. C 53 (1992) 127; Phys.Lett. B 306 (1993) 391.
- [5] F.M.Steffens and A.W.Thomas, Adelaide preprint ADP-94-27/T166.
- [6] T.Weigl and W.Melnitchouk, T.U.Munich preprint TUM/T39-95-9.
- [7] G.B.West, Los Alamos preprint LA-UR-91-3460; Phys.Rev.Lett. 67 (1991) 1388.
- [8] P.V.Landshoff, J.C.Polkinghorne and R.D.Short, Nucl.Phys. B 28 (1971) 225.
- [9] S.A.Kulagin, G.Piller and W.Weise, Phys.Rev. C 50 (1994) 1154.

- [10] A.Di Giacomo and H.Panagopoulos, Phys.Lett. B 285 (1992) 133.
- [11] A.I.Signal and A.W.Thomas, Phys.Rev. D 40 (1989) 2832; Phys.Lett. B 221 (1988) 481;
A.W.Schreiber, A.I.Signal and A.W.Thomas, Phys.Rev. D 44 (1991) 2653.
- [12] R.C.Hwa, Phys.Rev. D 22 (1980) 1593.
- [13] W.Zhu and J.G.Shen, Phys.Lett. B 219 (1989) 107; *ibid* B 235 (1990) 170.
- [14] K.Suzuki, T.Shigetani and H.Toki, Nucl.Phys. A 573 (1994) 541.
- [15] Y.Nambu and G.Jona-Lasinio, Phys.Rev. Phys.Rev. 122 (1961) 345.
- [16] S.Klimt, M.Lutz, U.Vogl and W.Weise, Nucl.Phys. A 516 (1990) 429; U.Vogl and
W.Weise, Prog.Part.Nucl.Phys. 27 (1991) 195; T.Hatsuda and T.Kunihiro, Phys.Rep.
247 (1994) 221; H.Reinhardt and R.Alkofer, Phys.Lett. B 207 (1988) 482.
- [17] F.E.Close and A.W.Thomas, Phys.Lett. B 212 (1988) 227.
- [18] H.Meyer, Phys.Lett. B 337 (1994) 37.
- [19] A.De Rujula and F.Martin, Phys.Rev. D 22 (1980) 1787.
- [20] H.Meyer and P.J.Mulders, Nucl.Phys. A 528 (1991) 589; P.J.Mulders, A.W.Schreiber,
and H.Meyer, Nucl.Phys. A 549 (1992) 498.
- [21] W.Melnitchouk, A.W.Schreiber and A.W.Thomas, Phys.Rev. D 49 (1994) 1183;
Phys.Lett. B 335 (1994) 11.
- [22] W.Melnitchouk, G.Piller and A.W.Thomas, Phys.Lett. B 346 (1995) 165.
- [23] W.Melnitchouk and W.Weise, Phys.Lett. B 334 (1994) 275.
- [24] N.Ishii, W.Bentz and K.Yazaki, Phys.Lett. B 301 (1993) 165; *ibid* B 318 (1993) 26.
- [25] S.Huang and J.Tjon, Phys.Rev. C 49 (1994) 1702.
- [26] A.Buck, R.Alkofer and H.Reinhardt, Phys.Lett. B 286 (1993) 29; G.Hellstern and

- C.Weiss, Phys.Lett. B 351 (1995) 64.
- [27] L.S.Celenza, C.M.Shakin, W.-D.Sun and J.Szweda, Phys.Rev. C 51 (1995) 937.
- [28] C.Stangl and W.Weise, in preparation.
- [29] L.S.Celenza, C.M.Shakin, W.-D.Sun, J.Szweda and X.-Q.Zhu, Phys.Rev. D 51 (1995) 3638.
- [30] A.D.Martin, R.Roberts and W.J.Stirling, Phys.Rev. D 50 (1994) 6734; CTEQ Collaboration, H.L.Lai *et al.*, Phys.Rev. D 51 (1995) 4763.
- [31] V.Bernard, R.L.Jaffe and U.-G.Meissner, Nucl.Phys. B 308 (1988) 753.
- [32] S.Weinberg, Phys.Rev. 150 (1966) 1313.
- [33] S.D.Drell, D.J.Levy and T.M.Yan, Phys.Rev. D 1 (1970) 1035.
- [34] W.Melnitchouk and A.W.Thomas, Phys.Rev. D 47 (1993) 3794; A.W.Thomas and W.Melnitchouk, in: Proceedings of the JSPS-INS Spring School (Shimoda, Japan) (World Scientific, Singapore, 1993).
- [35] A.Manohar and H.Georgi, Nucl.Phys. B 234 (1984) 189.
- [36] E.Eichten, I.Hinchliffe and C.Quigg, Phys.Rev. D 45 (1993) 2269.
- [37] T.Weigl and W.Weise, in preparation.
- [38] T.Shigetani, K.Suzuki and H.Toki, Phys.Lett. B 308 (1993) 383.
- [39] C.M.Shakin and W.-D.Sun, Phys.Rev. C 50 (1994) 2553.
- [40] V.R.Zoller, Z.Phys. C 54 (1992) 425.
- [41] U.Grandel and W.Weise, Phys.Lett. B (1995), in print.
- [42] A.Donnachie and P.V.Landshoff, Phys.Lett. B 296 (1992) 227.
- [43] S.A.Kulagin, W.Melnitchouk, G.Piller and W.Weise, Phys.Rev. C 52 (1995) 932.

[44] R.D.Ball and S.Forte, Nucl.Phys. B 425 (1994) 516.

FIGURES

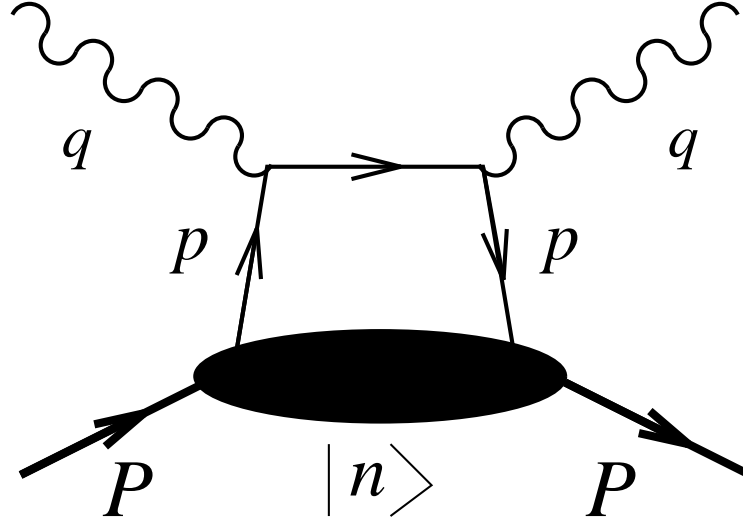


FIG. 1. Leading twist contribution to deep-inelastic scattering of a photon (momentum q) from a constituent quark (p) within a nucleon (P), with $|n\rangle$ labeling the spectator quark system.

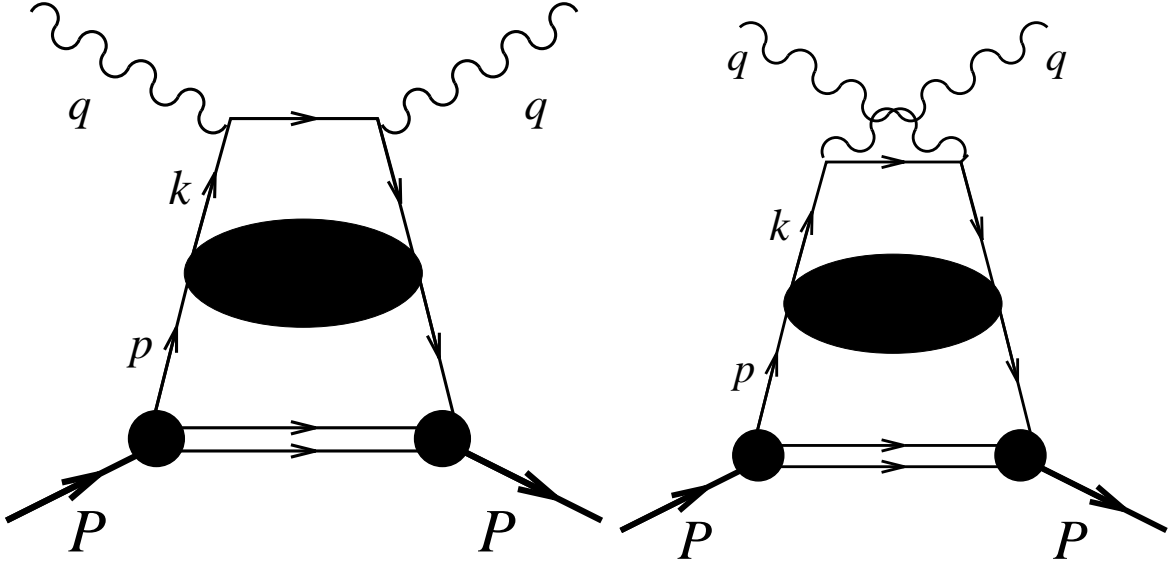


FIG. 2. DIS from a constituent quark with substructure. (a) direct photon diagram, which contributes to the quark distribution, (b) crossed photon diagram, associated with the antiquark distribution in the nucleon.

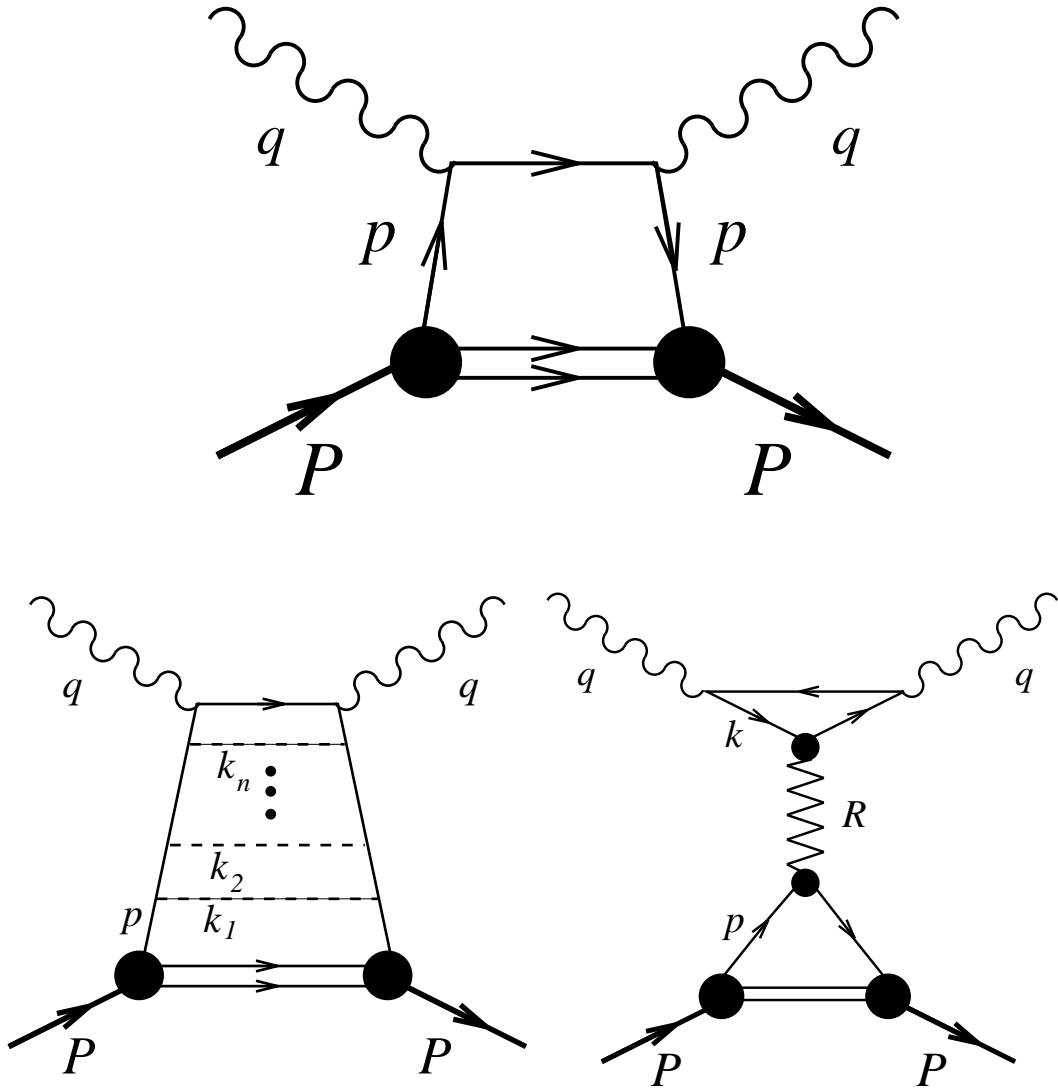


FIG. 3. Contribution to the nucleon structure function from the (a) low mass spectator (di-quark), (b) intermediate mass pion-exchange, and (c) large mass (asymptotic) components of the nucleon spectral function.

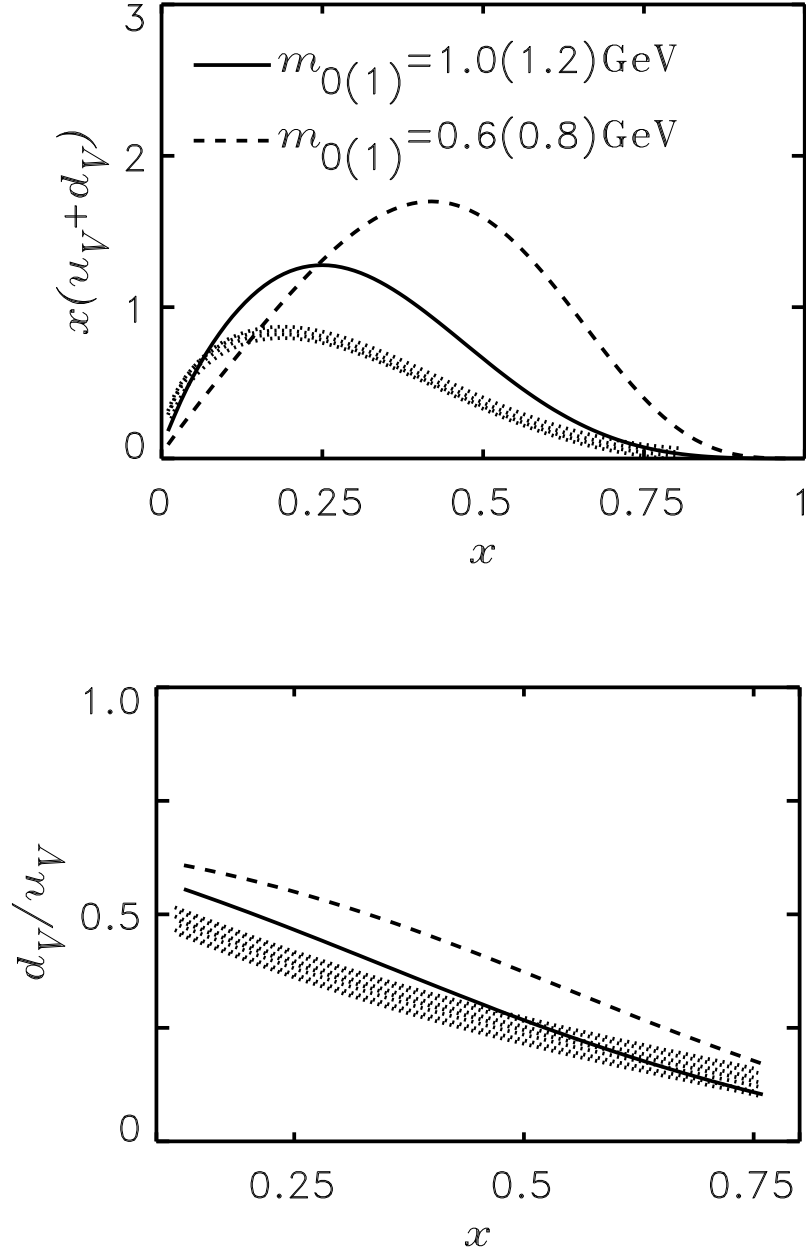


FIG. 4. (a) Total valence $x(u_V + d_V)$ quark distribution, and (b) valence d_V/u_V ratio, including only diquark spectators (process \mathcal{A}), with two sets of mass parameters, $m_{0(1)} = 1.0(1.2)$ GeV (solid) and $m_{0(1)} = 0.6(0.8)$ GeV (dashed). The curves are evolved from $\mu^2 = 1$ GeV² to $Q^2 = 10$ GeV², and the shaded area represents parametrizations of data taken from Ref. [30].

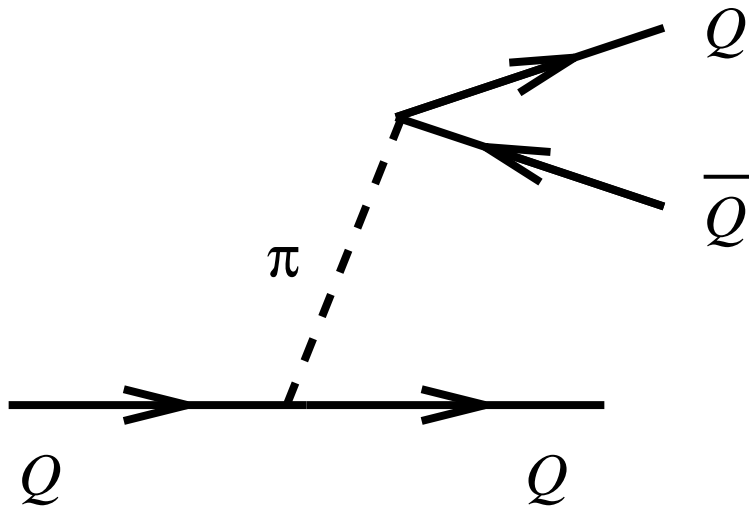


FIG. 5. Typical dissociation process generated from the effective constituent quark–pion interaction $\mathcal{L}_{Q\pi}$.

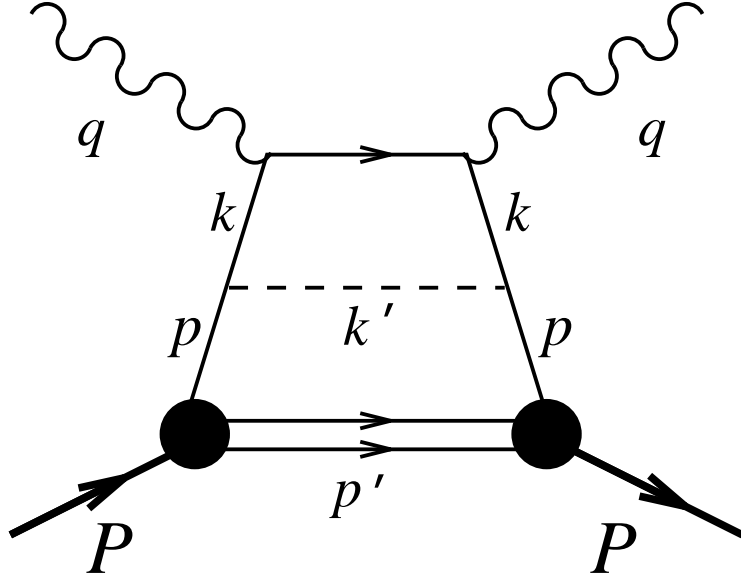


FIG. 6. One-pion exchange contribution to the quark distribution function.

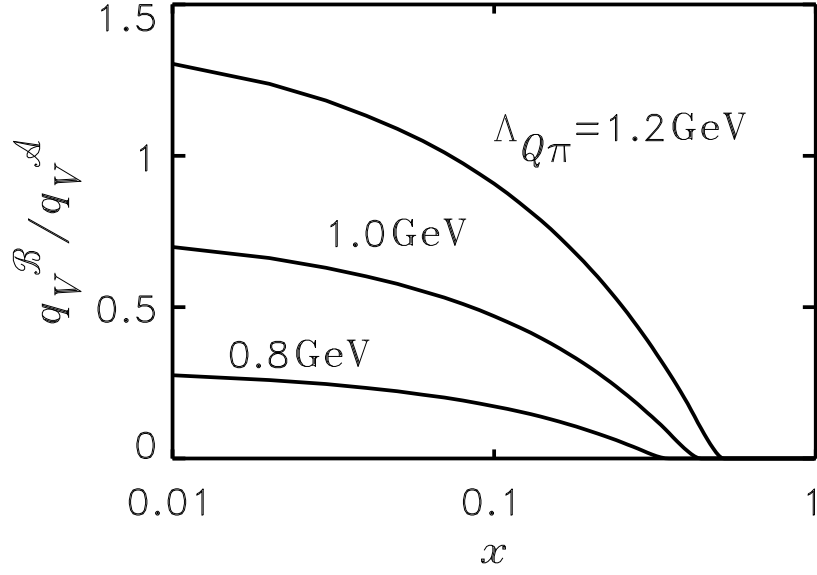


FIG. 7. Ratio of the one-pion exchange (\mathcal{B}) to the handbag contributions (\mathcal{A}) to the total valence distribution, $q = u_V + d_V$, for different $Q\pi$ vertex cut-off parameters.

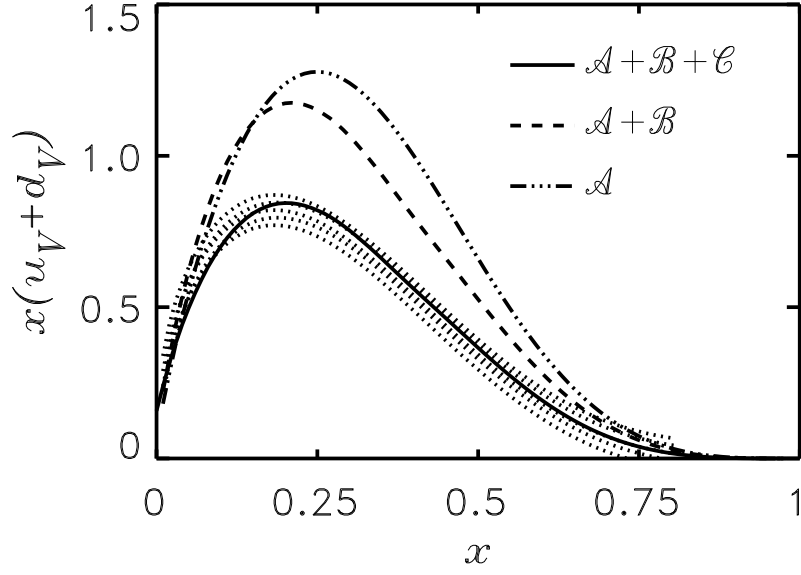


FIG. 8. Total valence quark distribution evolved from $\mu^2 = 1 \text{ GeV}^2$ to $Q^2 = 10 \text{ GeV}^2$, from process \mathcal{A} and \mathcal{B} , and \mathcal{A} alone (dashed), and from $\mathcal{A}-\mathcal{C}$ together (solid). Shaded region represents data at $Q^2 = 10 \text{ GeV}^2$.

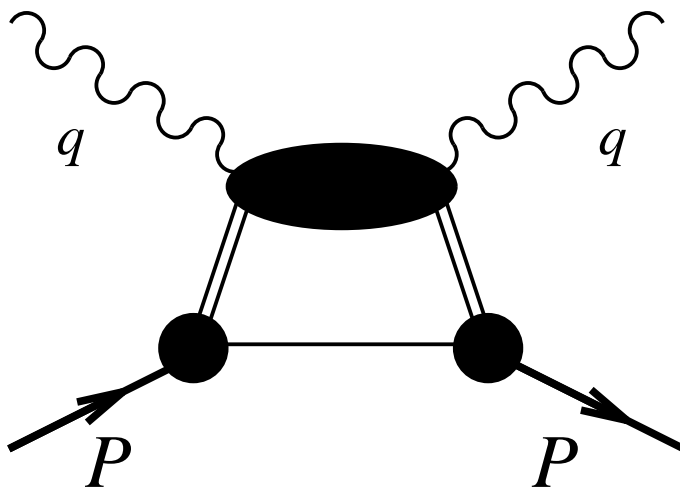


FIG. 9. Deep-inelastic scattering from a diquark in the nucleon.